Applied Physics Letters

# Room temperature ferrimagnetism in Yb-doped relaxor ferroelectric $PbFe_{2/3}W_{1/3}O_3$

Cite as: Appl. Phys. Lett. **115**, 072902 (2019); https://doi.org/10.1063/1.5112142
Submitted: 03 June 2019 . Accepted: 19 July 2019 . Published Online: 13 August 2019

D. C. Joshi, S. A. Ivanov, A. A. Bush, T. Sarkar, Z.-G. Ye, P. Nordblad, and R. Mathieu

Applied Physics Letters ARTICLE scitation.org/journal/apl

# Room temperature ferrimagnetism in Yb-doped relaxor ferroelectric $PbFe_{2/3}W_{1/3}O_3$

Cite as: Appl. Phys. Lett. **115**, 072902 (2019); doi: 10.1063/1.5112142
Submitted: 3 June 2019 · Accepted: 19 July 2019 ·
Published Online: 13 August 2019

View Online Export Citation CrossMark

D. C. Joshi,[1,a] S. A. Ivanov,[1,2] A. A. Bush,[3] T. Sarkar,[1] Z.-G. Ye,[4] P. Nordblad,[1] and R. Mathieu[1]

## AFFILIATIONS

[1]Department of Engineering Sciences, Uppsala University, Box 534, SE-751 21 Uppsala, Sweden
[2]Department of Inorganic Materials, Karpov Institute of Physical Chemistry, 105064 Moscow, Russia
[3]MIREA-Russian Technological University, 119454 Moscow, Russia
[4]Department of Chemistry and 4D LABS, Simon Fraser University, Burnaby, British Columbia V5A 1A6, Canada

[a]Author to whom correspondence should be addressed: deep.joshi@angstrom.uu.se

## ABSTRACT

We report ferrimagnetism and reentrant relaxor ferroelectricity near room temperature in a Yb-doped $PbFe_{2/3}W_{1/3}O_3$ cubic perovskite. Structural analysis reveals the presence of a single cubic perovskite phase, with the $Fm\bar{3}m$ space group [lattice parameter: $a = 8.0112(3)$ Å], and partial *B*-site ordering. The *B*-site ordering yields uncompensated magnetic moments in the antiferromagnetic structure of $PbFe_{2/3}W_{1/3}O_3$ and ferrimagnetism near room temperature. An excess moment of ~0.6 $\mu_B$/*B*-site may be estimated from magnetic hysteresis curves recorded up to 50 kOe at 5 K. The temperature dependent magnetodielectric study reveals a sequential phase transition from a long-range ferroelectric state (across 280 K) to a short-range relaxor ferroelectric state (across 190 K). The long-range ferroelectric ordering is found to be more affected by the application of external magnetic fields than the relaxor phase.



Multiferroic materials have gained enormous attention due to their technological potential in multifunctional devices such as sensors, transducers, memory devices, and spintronics.[1–3] There has been an extensive search for multiferroics, which can exhibit significant magnetoelectric effects at or above room temperature.[2,4] Such properties enable a wide range of applications like magnetoelectric memory and voltage-tunable spintronic devices.[1–3,5] In this context, the Pb based double perovskite $PbFe_{2/3}W_{1/3}O_3$ (PFWO) and its solid solutions are considered as promising candidates for displaying the desired room-temperature polar and magnetic ordering.[6–9] Recent studies on the solid solution system $Pb(Fe_{1-x}A_x)_{2/3}W_{1/3}O_3$ ($0 \le x \le 1$, where A is the magnetic or nonmagnetic cations) found a strong dependency of cation ordering (splitting of the *B*-site into *B′* and *B″* sites) on the doping concentration.[9,10] At this point, it is worth noting the effect of magnetic and nonmagnetic substitution of Fe on the global magnetic and dielectric properties of PFWO. First, the addition of a magnetic cation such as $Mn^{3+}$ seems to hinder the long range magnetic ordering.[9] In contrast, the magnetic dilution by incorporating nonmagnetic cations, e.g., $Sc^{3+}$ in PFWO [$Pb(Fe_{1-x}Sc_x)_{2/3}W_{1/3}O_3$ ($0 \le x \le 1$, PFSWO)], leads to cation ordering between B′ and B″ sites. Such cationic order gives rise to uncompensated moments and switches the antiferromagnetic ordering to ferrimagnetic ordering, while the relaxor ferroelectric properties seemingly remain unaffected.[11] In spite of the improved magnetic properties, PFSWO requires special heat treatment conditions in order to obtain solely the *B*-site cation ordered phase stability over the entire composition range.[11] Considering these particulars, we here replace the magnetic $Fe^{3+}$ cations by an 4*f*-element $Yb^{3+}$ cation, $Pb(Fe_{1-x}Yb_x)_{2/3}W_{1/3}O_3$ ($0 \le x \le 1$, PFYWO), $Yb^{3+}$ having a larger ionic radius (0.868 Å) as compared to $Fe^{3+}$ (0.645 Å) and $Sc^{3+}$ (0.745 Å).[12] All the synthesized samples are perfectly ordered without any special heat treatment. Interesting results are observed for the composition of $x = 10\%$, which exhibits the coexistence of the relaxor ferroelectric state and room temperature ferrimagnetic ordering and is the main focus of this study. The ceramic sample of $Pb(Fe_{0.9}Yb_{0.1})_{2/3}W_{1/3}O_3$ was prepared by the conventional mixed-oxide route. High purity powders PbO (99.99% purity), $Fe_2O_3$ (99.98% purity), $WO_3$ (99.9%), and $Yb_2O_3$ (99.9% purity) have been used as starting materials. For compensation of Pb evaporation during sintering, 5% extra weight of PbO has been added. The mixtures of oxides were ball-milled for a period of 2 h. The powders were successively dried, pressed into disks, and then sintered at 1173 K (12 h). In the next step, the obtained pellets have been crushed and milled in a

mortar. The obtained powders were uniaxially pressed into disks with a diameter of 10 mm and a thickness of about 3 mm, using polyvinyl alcohol as a binder. Such prepared disks have been sintered in alumina crucibles at 1273 K for 3 h, with the heating rate of about 2.5 K/min. Finally, the obtained ceramic samples were ground, polished, and annealed at a temperature of 973 K (in order to remove mechanical stresses) and slowly cooled down to room temperature. The crystal structure and chemical purity of the above synthesized samples were studied by using a Bruker D8 Advance diffractometer (Vantec position-sensitive detector, Ge-monochromatized Cu $K\alpha$ radiation, Bragg-Brentano geometry, and DIFFRACT plus software) in the $2\theta$ range of 10°–152° with a step size of 0.02° (the counting time was 15–20 s per step). The chemical composition, stoichiometry, and homogeneity of the samples were analyzed by energy-dispersive spectroscopy (EDS) using a JEOL 840A scanning electron microscope and INCA 4.07 (Oxford Instruments) software. The magnetodielectric measurements were performed in the temperature range of 10 K–400 K and frequency range of 1 kHz–430 kHz, using an Agilent E4980 precision LCR meter and a customized physical property measurement system (PPMS) probe. Both the sides of the samples were polished by fine sand paper and coated with conductive silver paint followed by slow drying before carrying out the experiments. The temperature and magnetic field dependent magnetization of the samples were measured using a superconducting quantum interference device (SQUID) magnetometer from Quantum Design Inc. The dependence of the magnetization on temperature was recorded in zero-field cooled (ZFC) and field cooled (FC) conditions under magnetic fields $H_{dc}$ of 100 Oe and 1000 Oe. Magnetic hysteresis curves were recorded at different temperatures for magnetic fields up to ±50 kOe. Ferroelectric hysteresis loops were measured at 130 K (below the ferroelectric Curie point) by using a Sawyer-Tower circuit at a frequency of 400 Hz.

Figure 1 shows the X-ray diffraction (XRD) pattern of the $Pb(Fe_{0.9}Yb_{0.1})_{2/3}W_{1/3}O_3$ polycrystalline sample together with its Rietveld refinement data, which confirms the presence of the ordered cubic perovskite phase having space group $Fm\bar{3}m$ with a lattice parameter of $a = 8.0112(3)$ Å. An additional superstructure reflection at

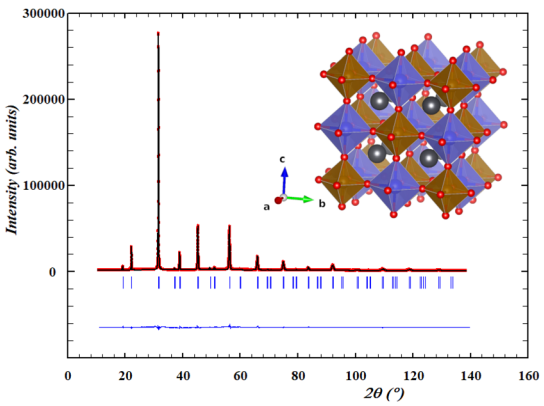


**FIG. 1.** X-ray diffraction pattern together with final Rietveld refinement of polycrystalline $Pb(Fe_{0.9}Yb_{0.1})_{2/3}W_{1/3}O_3$ with $R_p$, $R_{wp}$, $R_B$, and $\chi^2$ values of 3.98, 5.13, 3.16, and 2.16, respectively. The inset shows the polyhedral representation of the crystal structure, drawn using VESTA;[13] $Pb^{2+}$ ions are drawn in gray, oxygen anions in red, and the $Fe(W)O_6$ and $Fe(Yb)O_6$ octahedra in violet and orange, respectively.

$2\theta = 19.00°$ was observed signifying the development of stoichiometric *B*-site cation ordering.[9,11,14] In the case of PFYWO, no quenching procedure akin to that used in the Sc case[11] was necessary, and a single $Fm\bar{3}m$ phase is obtained without fractions of disordered $Pm\bar{3}m$. The cationic concentrations (at. %) of the sample determined from the EDS analysis are found to be rather close to the stoichiometric composition: Pb = 49.8(2), Fe = 30.3(2), Yb = 3.1(2), and W = 16.8(2), which correspond to the chemical formula: $PbFe_{0.61}Yb_{0.06}W_{0.33}O_3$. The occupancies, which we have determined, lead to the chemical formula: $Pb_{7.91(4)}[Fe_{1.84(4)}Yb_{0.17(4)}W_{1.99(4)}]_{4a}$ $[Fe_{2.97(4)}Yb_{0.36(4)}W_{0.67(4)}]_{4b}O_{24}$. Figures 2(a) and 2(b) show the temperature dependence of the zero-field cooled (ZFC) and field cooled (FC) magnetization M(T) curves for $Pb(Fe_{0.9}Yb_{0.1})_{2/3}W_{1/3}O_3$ and pure $PbFe_{2/3}W_{1/3}O_3$ ceramic samples recorded at a constant dc-field $H_{dc}$ of 100 Oe, respectively. To record the ZFC magnetization, the sample was first cooled to a low temperature in the absence of a magnetic field, where a $H_{dc}$ value of 100 Oe was applied and the ZFC magnetization recorded on warming the sample. The FC data were recorded on warming, after cooling the sample in $H_{dc}$. The M(T) curve for $Pb(Fe_{0.9}Yb_{0.1})_{2/3}W_{1/3}O_3$ exhibits a sharp rise in magnetization close to room temperature. This is in sharp contrast to the undoped PFWO ceramic. The ZFC and FC curves exhibit some irreversibility reflecting the temperature dependence of the coercivity of the excess moment that appears below $T_N$.[9] On the other hand, undoped PFWO ceramics and single crystals exhibit an antiferromagnetic transition near 340 K as shown in Fig. 2(b). This antiferromagnetic transition is much sharper and clearer in single crystal PFWO as compared to ceramic PFWO [inset of Fig. 2(b)]. Thus, incorporation of 10% Yb at the *B*-site of PFWO changes the nature of magnetic ordering and brings the ordering temperature closer to room temperature. The total magnetic moment in an ideal AFM structure with *B*-site disorder shall be close to zero, but in the case of PFYWO, the two magnetic sublattices are nonequivalent and noncompensated. The field dependence of magnetization M(H) curves for single crystal and polycrystalline PFWO and polycrystalline $Pb(Fe_{0.9}Yb_{0.1})_{2/3}W_{1/3}O_3$ measured at a constant temperature of T ~ 5 K are shown in Fig. 2(c). For $x = 0$, the system exhibits a relatively low value of magnetization (~0.14 $\mu_B$ at H = 50 kOe). The incorporation of 10% Yb at the *B*-site of PFWO leads to excess magnetization M (~0.63 $\mu_B$ at H = 50 kOe) due to unbalanced magnetic sublattices below the ordering temperature. Considering the occupancies on the two respective *B*-sites as determined by X-ray data for Fe, W, and Yb in PFYWO and magnetic moment 5 $\mu_B$ per $Fe^{3+}$, we expect an excess moment of ~0.60 $\mu_B$ which is in good agreement with the value obtained from the field dependent magnetization curves [Fig. 2(d)]. Figure 2(d) shows the field dependence of magnetization M(H) recorded at four different temperatures (i) 5 K, (ii) 200 K, (iii) 250 K, and (iv) 300 K for $x = 0.10$. The nonlinearity persists until 300 K, showing the presence of magnetic ordering at room temperature. The dependence of M on temperature measured at high fields (H = 1 T, 1.5 T, 2 T, and 3 T) is depicted in the inset of Fig. 2(d) from which we can notice the loss of irreversibility. Using the temperature dependent M(T) data at high fields, we have calculated the change in magnetic entropy ΔS by simply considering $\Delta S \approx dM/dT \times \mu_0 H$, which yielded $\Delta S = 0.03$ J/kg K at T = 286 K.[15,16]

Figure 3 shows the temperature dependence of dielectric permittivity $\varepsilon_r(T)$ and dielectric loss tangent $\tan\delta(T)$ for the $Pb(Fe_{0.9}Yb_{0.1})_{2/3}W_{1/3}O_3$

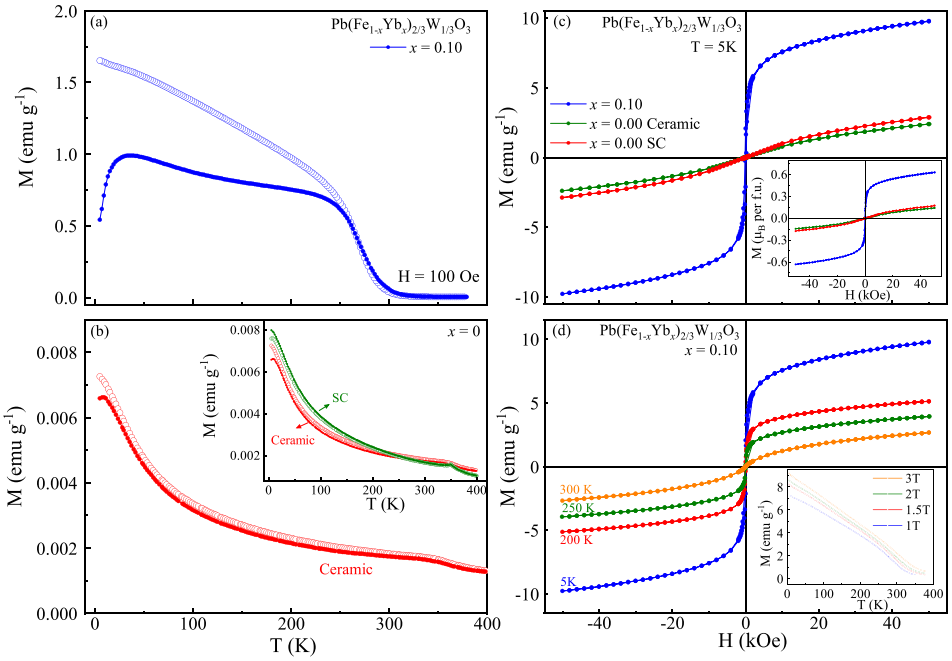


**FIG. 2.** Temperature dependence of magnetization M(T) for (a) $Pb(Fe_{0.9}Yb_{0.1})_{2/3}W_{1/3}O_3$ and (b) pure $PbFe_{2/3}W_{1/3}O_3$ ceramic samples recorded at a constant dc-field $H_{dc}$ of 100 Oe under zero-field cooled (ZFC) and field cooled (FC) conditions as shown by solid filled and hollow symbols, respectively. The inset shows the M(T) curve for the $PbFe_{2/3}W_{1/3}O_3$ ceramic (red color) and single crystal (green color) measured at $H_{dc} = 100$ Oe. The field dependence of magnetization M(H) for (c) single crystal and polycrystalline line $PbFe_{2/3}W_{1/3}O_3$ and polycrystalline $Pb(Fe_{0.9}Yb_{0.1})_{2/3}W_{1/3}O_3$ measured at a constant temperature of T = 5 K (reported in $\mu_B$ per f.u. in the inset) and (d) polycrystalline $Pb(Fe_{0.9}Yb_{0.1})_{2/3}W_{1/3}O_3$ measured at four different temperatures of T = 5 K, 200 K, 250 K, and 300 K. The inset of (d) shows the M(T) curves measured at four different magnetic fields H = 1 T, 1.5 T, 2 T, and 3 T under field cooled conditions for polycrystalline $Pb(Fe_{0.9}Yb_{0.1})_{2/3}W_{1/3}O_3$.

ceramic measured at various frequencies ranging between 1 kHz and 430 kHz, and the data were taken during the heating cycle (no significant change was noticed for the cooling cycle). Interestingly, $\varepsilon_r$(T) exhibits a twin peak behavior between the temperatures of 172 K and 340 K. On the one hand, the first peak at 192 K ($f = 1$ kHz) shows a frequency dispersion in which the dielectric maximum $\varepsilon_m$ shifts toward higher temperature from 192 K to 212 K with increasing frequency $f$ from 1 kHz to 430 kHz, and such an increase is a typical characteristic of relaxor ferroelectrics.[17] The second peak observed at 280 K does not exhibit any frequency dependence, which signifies the

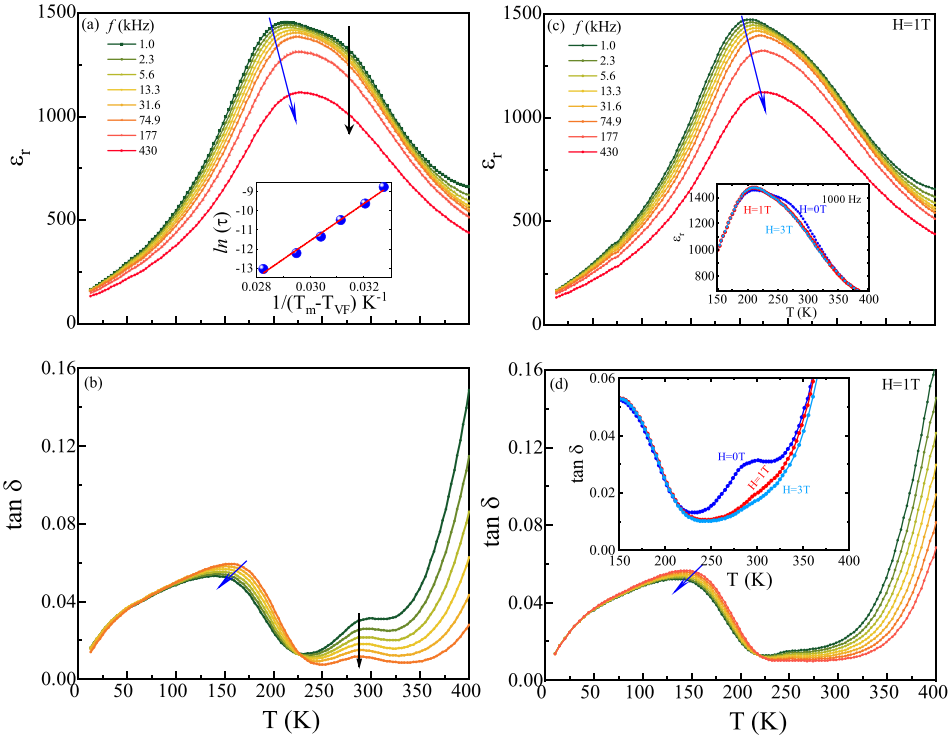


**FIG. 3.** Temperature dependence of (a) dielectric permittivity $\varepsilon_r$(T) and (b) loss tangent $\tan\delta$(T) for polycrystalline $Pb(Fe_{0.9}Yb_{0.1})_{2/3}W_{1/3}O_3$ measured at various frequencies ranging between 1 kHz and 430 kHz. (c) and (d) show the results of the same measurements in the presence of a constant magnetic field $H_{dc} = 1$ T. The circular symbols in the inset of (a) show the logarithmic variation of $\tau$ as a function of $1/(T_m - T_{VF})$, and the solid continuous line is the best fit to the Vogel-Fulcher equation. The insets of (c) and (d) show the zoomed view of $\varepsilon_r$(T) and $\tan\delta$(T) recorded at three different dc-magnetic fields $H_{dc} = 0$ T, 1 T, and 3 T and measured at a constant frequency of 1 kHz.

presence of a long-range ferroelectric phase associated with PFWO.[18,19] The long-range ferroelectric ordering can be further confirmed from the hysteresis observed in the polarization vs electric field loop (P-E loop) recorded at a frequency of 400 Hz and a temperature of 130 K, as shown in the supplementary material figure. Thus, when the temperature decreases, the system undergoes a sequential phase transition from a long-range ferroelectric phase to a short-range relaxor ferroelectric state. Such a behavior is characteristic of the so-called reentrant ferroelectric relaxors.[18,19] Moreover, the frequency dependence of $T_m$ follows the Vogel-Fulcher (VF) law [inset of Fig. 3(a)] as given by the following equation:[17]

$$\tau = \tau_0 \exp\left[\frac{E_a}{k_B(T_m - T_{VF})}\right], \quad (1)$$

where $E_a$ (=0.04 eV) is the activation energy, $T_{VF}$ (=174 K) is the freezing temperature of the polarization function, $k_B$ is the Boltzmann constant, and the pre-exponential factor $\tau_0$ (=$7.85 \times 10^{-12}$ s) is known as the characteristic relaxation time. The observed parameters are in good agreement with lead magnesium niobate ($\tau_0 = 1.54 \times 10^{-13}$ s and $E_a = 0.0407$ eV), which is a typical example of a classical relaxor ferroelectric.[20] In addition, these values are also consistent with the previously reported values of pure PFWO; $\tau_0$ and $E_a$ are $2.57 \times 10^{-11}$ s and 0.0396 eV in Ref. 10 and $4.08 \times 10^{-14}$ s and 0.06 eV in Ref. 9 for $Pb[(Fe_{2/3W}^{1/3})_{1-x}Mn_x]O_3$ ($0 \le x \le 0.02$) (PFMWO); $\tau_0$ and $E_a$ are $2.44 \times 10^{-12}$ s and 0.0390 eV in Ref. 10. The presence of oxygen vacancies, characteristic of lead-based perovskite, causes the relaxation maxima in the $\varepsilon_r$(T) and tan $\delta$(T) dependences in the temperature range of 250–700 K.[21] For lead ferrotungstate $PbFe_{2/3}W_{1/3}O_3$ and its solid solutions, such maxima are often observed in the range of 250–400 K.[9,10,22] However, we did not notice the high temperature Debye-like relaxation as observed in Ref. 9 for PFWO, suggesting a defect (i.e., oxygen vacancies) free PFYWO sample. The dispersion of the dielectric constant observed at high temperatures is apparently due to the increased conductivity of the sample. The applied electric field leads to asymmetry in the distribution of moving charges (electrons, ions, or dipoles), which in turn causes the emergence of the so-called thermal or relaxation contribution to the polarization of the sample.[23] It is interesting that the application of external magnetic field $H_{dc}$ significantly suppressed the twin peak behavior as shown in Figs. 3(c) and 3(d) and their corresponding insets. As $H_{dc}$ increases from 0 T to 3 T, $\varepsilon_r$ (280 K) decreases from 1308 to 1285, while $\varepsilon_r$ (208 K) increases from 1453 to 1474. It appears that the relaxor state is weakly affected by the magnetic field, while the "ferroelectriclike" behavior is suppressed.

In summary, the structural analysis reveals a cubic perovskite phase (space group: $Fm\bar{3}m$) with partial *B*-site ordering for 10%Yb-doped $PbFe_{2/3}W_{1/3}O_3$. The observed behavior of the temperature and field dependent magnetization suggests a switching of the magnetic ordering from antiferromagnetic to ferrimagnetic after the incorporation of Yb in $PbFe_{2/3}W_{1/3}O_3$. The excess *B*-site moment (~0.6 $\mu_B$) determined from the low temperature magnetization data is in good agreement with the value obtained by considering the respective occupancies of the $Fe^{3+}$ cations (carrying 5 $\mu_B$) on the two *B*-sites of the structure, determined by X-ray data. The temperature and field dependent dielectric study provides signatures of reentrant relaxor behavior, with ferroelectriclike ordering near 280 K and relaxor behavior at ~190 K. The frequency dispersion in the dielectric constant $\varepsilon_r$(T) associated with the short-range relaxor ferroelectric state is analyzed by means of the Vogel-Fulcher law, yielding the activation energy $E_a$ ~0.04 eV, the freezing temperature $T_{VF}$ ~174 K, and the characteristic relaxation time $\tau_0 \sim 7.85 \times 10^{-12}$ s, which are consistent with the corresponding values for standard classical relaxors. The effect of the magnetic field onto the temperature dependence of $\varepsilon_r$(T) is discussed.

See the supplementary material for (Fig. S1) the polarization vs electric field loop (P-E loop) recorded at a frequency of 400 Hz and a temperature of 130 K for the $Pb(Fe_{0.9}Yb_{0.1})_{2/3}W_{1/3}O_3$ polycrystalline sample. The hysteresis observed in the P-E loop recorded at 130 K (below the ferroelectric Curie point) provides the signature of long range ferroelectric ordering.

We thank the Stiftelsen Olle Engkvist Byggmästare, the Swedish Research Council (VR), Russian Foundation for Basic Research (No. 18-03-00245), and the Natural Sciences & Engineering Research Council of Canada (NSERC, Grant No. 203773) for financially supporting this work. T.S. acknowledges financial support from the VR starting Grant No. 2017-05030.

## REFERENCES

[1]M. Fiebig, T. Lottermoser, D. Meier, and M. Trassin, Nat. Rev. Mater. **1**, 16046 (2016).
[2]N. A. Spaldin, MRS Bull. **42**, 385 (2017).
[3]N. A. Spaldin and R. Ramesh, Nat. Mater. **18**, 203 (2019).
[4]Y. Tokura, S. Seki, and N. Nagaosa, Rep. Prog. Phys. **77**, 76501 (2014).
[5]R. Ramesh and N. A. Spaldin, Nat. Mater. **6**, 21 (2007).
[6]Z.-G. Ye and H. Schmid, Ferroelectrics **162**, 119 (1994).
[7]H. Liu and X. Yang, Ferroelectrics **507**, 69 (2017).
[8]G. A. Smolenskii, A. I. Agranovskaya, and V. A. Isupov, Sov. Phys.-Solid State **1**, 907 (1959).
[9]S. A. Ivanov, A. A. Bush, C. Ritter, M. A. Behtin, V. M. Cherepanov, C. Autieri, Y. O. Kvashnin, I. D.Marco, B. Sanyal, O. Eriksson, P. A. Kumar, P. Nordblad, and R. Mathieu, Mater. Chem. Phys. **187**, 218 (2017).
[10]L. Zhou, P. M. Vilarinho, and J. L. Baptista, J. Appl. Phys. **85**, 2312 (1999).
[11]S. A. Ivanov, P. Beran, A. A. Bush, T. Sarkar, S. Shafeie, D. Wang, O. Eriksson, M. Sahlberg, Y. Kvashnin, R. Tellgren, P. Nordblad, and R. Mathieu, Eur. Phys. J. B **92**, 163 (2019).
[12]R. D. Shannon, Acta Crystallogr., Sect. A **32**, 751 (1976).
[13]K. Momma and F. Izumi, J. Appl. Crystallogr. **44**, 1272 (2011).
[14]R. Wongmaneerung, X. Tan, R. W. McCallum, S. Ananta, and R. Yimnirun, Appl. Phys. Lett. **90**, 242905 (2007).
[15]S. A. Ivanov, M. S. Andersson, J. Cedervall, E. Lewin, M. Sahlberg, G. V. Bazuev, P. Nordblad, and R. Mathieu, J. Mater. Sci. **29**, 18581 (2018).
[16]M. Hudl, R. Mathieu, P. Nordblad, S. A. Ivanov, G. V. Bazuev, and P. Lazor, J. Magn. Magn. Mater. **331**, 193 (2013).
[17]A. A. Bokov, M. A. Leshchenko, M. A. Malitskaya, and I. P. Raevski, J. Phys. Condens. Matter **11**, 4899 (1999).
[18]V. V. Shvartsman and D. C. Lupascu, J. Am. Ceram. Soc. **95**, 1 (2012).
[19]A. A. Bokov and Z.-G. Ye, Nanoscale Ferroelectr. Multiferroics **1**, 729 (2016).
[20]D. Viehland, S. J. Jang, L. E. Cross, and M. Wuttig, J. Appl. Phys. **68**, 2916 (1990).
[21]B. S. Kang, S.-K. Choi, and C. H. Park, J. Appl. Phys. **94**, 1904 (2003).
[22]A. F. Koroleva, A. A. Bush, K. E. Kamentsev, V. Y. Shkuratov, S. A. Ivanov, V. M. Cherepanov, and S. Shafeie, Inorg. Mater. **54**, 288 (2018).
[23]A. K. Jonscher, *Dielectric Relaxation in Solids* (Chelsea, 1983).